Journal of the Ceramic Society of Japan 120 [2] 64-68 2012 Paper

Characterization of microstructures of thermal oxide scales on silicon carbide using transmission electron microscopy

Bralee CHAYASOMBAT, Takeharu KATO,* Tsukasa HIRAYAMA,* Tomoharu TOKUNAGA, Katsuhiro SASAKI**,† and Kotaro KURODA****

National Metal and Materials Technology Center, Thailand Science Park, Klong Luang, Pathumthani, 12120, Thailand
***Nanostructures Research Laboratory, Japan Fine Ceramics Center, Atsuta-ku, Nagoya 456–8587, Japan**
****Department of Quantum Engineering, Nagoya University, Furo-cho Nagoya 464–8603, Japan**

Hexagonal single crystal silicon carbide was thermally oxidized in pure oxygen and in air at 1473 K. The thermally formed oxide scales were composed mostly of amorphous silica. However, some crystalline phase oxide scales were observed randomly distributed on the formed oxide scale. The ratio of crystalline scale to overall oxide scale was less than 5 percent. We characterized the microstructures of the thermally formed oxide scales using transmission electron microscopy with low-dose observation technique. The oxide scales in some regions were divided into two layers, with crystalline scale on the upper and amorphous scale on the lower layer. Traces of calcium were found in the crystalline phase oxide scale, which could have influenced the crystallization.

Key-words : 6H-SiC, Single crystal, Amorphous silica, Crystallization, Cross-sectional TEM, Ca impurity

[Received October 11, 2011; Accepted November 17, 2011]

1. Introduction

Silicon Carbide (SiC) has many desirable properties, such as high sublimation temperature, high chemical stability, and high thermal conductivity. These properties make it suitable for use as a structural material at high temperature and in harsh environments. Moreover, it also possesses excellent electrical properties, such as wide band gap and high break down electric field strength, which make it an attractive candidate for replacing silicon as a high power, high frequency, high efficiency and high temperature semiconductor device material.

Protective silica oxide scales are known to form on SiC at high temperature in an environment with sufficient oxygen partial pressure.[1] As for the morphology of the formed oxide scale, studies have reported finding crystalline oxide scale in the case of oxidation at relatively high temperature (above 1473 K) and sufficiently long oxidation time.[2)–7)] The most often reported crystalline phase silica has been alpha and beta phase of cristobalite. Some studies also reported the finding of a small amount of tridymite.[4),6)] The often reported cristobalite was mostly found as a thin disk-shaped structure in the amorphous silica matrix.[7)] This disk-shaped structure is referred to in many studies as spherulitic or rosettes cristobalite. As the oxidation advanced, these spherulitic crystals were reported to fall off.[5)] These fall-offs lead to the exposure of new un-oxidized surfaces of SiC, and the oxidation of SiC in that region will be accelerated and oxidized further compared to the surrounding regions. Therefore, in the case where SiC is used in a high temperature environment with repeated heating, annealing and cooling processes, the formation of these spherulitic crystalline oxide scales must be seriously considered. And in cases where SiC is used in electrical devices, the crystalline oxide scales will have an affect on the electrical properties of the insulating oxide layer. This will have a major effect on the performance of the device.

Therefore, it is important to understand the factors that influence the crystallization of the silica oxide scales. Also, a close study of the microstructures of oxide scales will lead to a deeper understanding of the crystallization processes. This understanding of the process may lead to the control and restriction of the crystallization of the silica scales.

In this study, we used optical microscopy (OM), scanning electron microscopy (SEM), and transmission electron microscopy (TEM) together with X-ray energy dispersive spectroscopy (XEDS) installed with TEM, to characterize the microstructures of the thermally formed crystalline oxide scale on single crystal SiC, in order to understand more about the microstructures and formations of the crystalline oxide scales.

2. Experimental procedures

The single crystal 6H-SiC wafer (n-type) used in this study was provided by Cree Inc. The wafer was polished on both the Si-face and the C-face. Then it was cut into $10 \times 10\,mm^2$ size pieces and rinsed in acetone and then successively cleaned ultrasonically in ethanol. The samples were then loaded onto a quartz sample holder and put into the quartz tube furnace.

The effects of contaminations from alumina furnace tubes on the oxidation of silicon carbide were reported by E. Opila.[8)] Accordingly, the level of contaminations in our experiments has been carefully controlled. The SiC sample used in this study was high purity single crystal 6H-SiC wafer and the furnace tube used in the oxidation experiment was a high quality quartz tube with quartz sample holder. The selection of the experimental samples and the experimental settings was to minimize the effects from contaminations on the oxidation.

Pure dry oxygen was introduced at a flow rate of approximate 100 cc/min for 2 h prior to the oxidation to ensure a pure dry oxygen environment. The furnace system was then heated up

† Corresponding author: K. Sasaki; E-mail: khsasaki@nagoya-u.jp

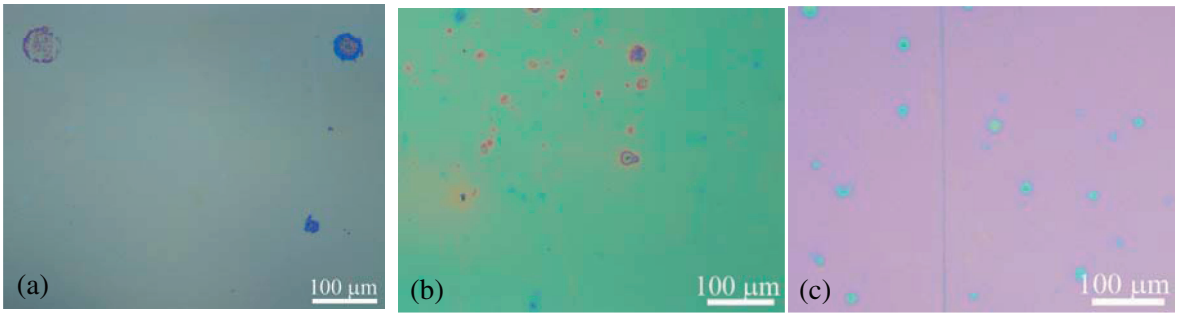

Fig. 1. OM image of the Si-face of samples after oxidized at 1473 K for (a) 9, (b) 16, and (c) 25 h, respectively.

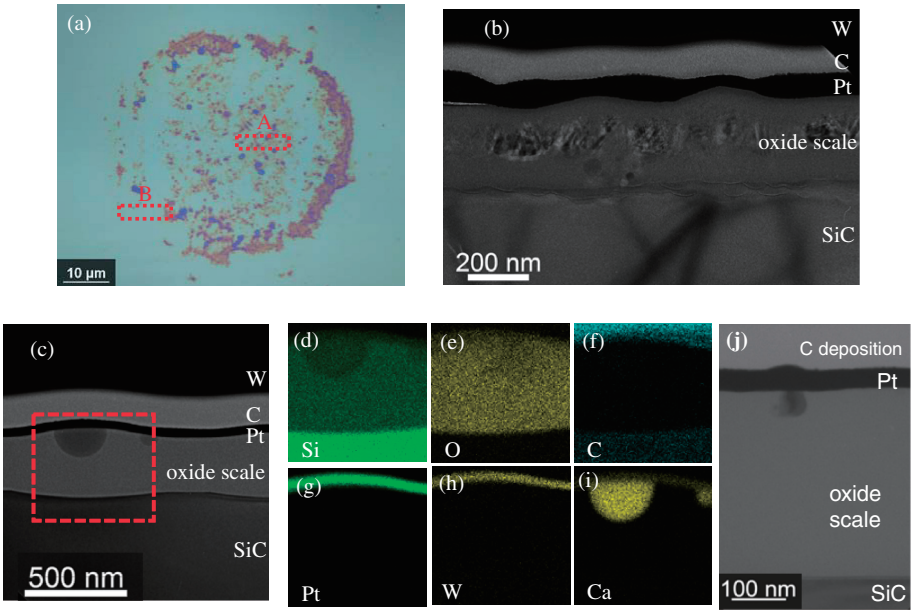

Fig. 2. (a) OM image of the sample after oxidized for 9 h, (b), (c) cross-sectional TEM images of region A and region B correspond to the regions indicated in (a). (d)–(i) XEDS elemental maps of Si, O, C, Pt, W and Ca, correspond to the region indicated by the broken-line square in (c), respectively. (j) The structure corresponding to (c) observed in C-face oxide scale.

at the rate of 10 degrees/min. The oxidation temperature was 1473 K with oxidation time from 9 to 25 h in flowing dry oxygen at 1 atm. Comparative experiments of oxidation were also conducted in air at ambient pressure.

The oxidized samples were then observed using OM. The regions with glossy color patterns, which were observed randomly scattered on the surface of the samples after thermal oxidation, were identified and marked using silver paste, then platinum was deposited on the surfaces of the samples to prevent electrical charging during TEM specimen preparation. TEM specimens were prepared by the focused ion beam (FIB) micro-sampling technique using a HITACHI NB-5000 FIB–SEM system at an accelerating voltage of 5–40 kV. Carbon and tungsten were also deposited on the surfaces of the samples in the FIB system prior to the TEM specimen preparation in order to protect the surfaces of the specimens from damage by FIB fabrication. The cross-sectional TEM specimens were observed in a JEM-2010 at an accelerating voltage of 200 kV. The crystalline phase of the oxide scale was highly sensitive to the electron beam irradiation. Accordingly, TEM low dose observation technique must be applied. XEDS spectrums and mapping was measured in a Topcon-002B at an accelerating voltage of 200 kV.

3. Results

Figure 1 shows OM images of the Si–face of the samples after oxidation at 1473 K for (a) 9 h (b) 16 h and (c) 25 h, respectively. The differences in color of the oxidized samples with different oxidation time are due to differences in the thickness of the formed oxide scale. Randomly scattered patterns with different color are observed from the majority of the oxide scales on the surface of the formed oxide scales of the samples for all oxidation times. The shape of the formed patterns was mostly round with rough edges. These spherical patterns are also random in size for all of the oxidation times. The sizes of the formed spherical patterns varied from a few micrometers to over a hundred micrometers in diameter. For the sample oxidized for 25 h [Fig. 1(c)], a scratch, which existed on the surface of the sample prior to the thermal oxidation, was observed. However, the spherical patterns did not form exclusively over this pre-existing scratch.

Figure 2(a) shows a high magnification OM image of one of the patterns formed on sample oxidized for 9 h. The diameter of the pattern is approximately 50 μm in size. Figure 2(b) shows cross-sectional TEM image of the specimen taken from region A indicated in Fig. 2(a). In this region, the oxide scale was

composed of both crystalline and amorphous silica scales. The thickness of the oxide scale in this region is not uniform. The cross-sectional TEM image of the specimen from region B, the region close to the edge of the spherical pattern, is shown in Fig. 2(c). In this region, the oxide scale is composed of only amorphous silica. However, the thickness of the oxide scale is not completely uniform in this region. Round-shape amorphous structures with darker contrast were observed in the amorphous oxide layer. Figures 2(d)–2(i) show the results of XEDS elemental mapping of this region. The corresponding round-shape structure has been observed on the C-face oxidized for 16 h at 1273 K, however, which was already crystallized as shown in Fig. 2(f).

Figure 3(a) shows OM images of the patterns formed on the sample oxidized for 16 h. The diameter of the pattern is approximately 20 micrometers in size. Figure 3(b) shows cross-sectional TEM image of the specimen taken from the region A indicated in Fig. 3(a). The oxide scale was composed of both amorphous and crystalline silica. Figure 3(c) shows a SADP taken from the region indicated by the broken-line circle in Fig. 3(b). From the SADP, the crystalline oxide scale was identified as polycrystalline tetragonal cristobalite (alpha cristobalite). Figure 3(d) shows cross-sectional TEM image from the surrounding region of the pattern indicated as the region B. In this surrounding region, the oxide scale is uniformly formed and composed of only amorphous silica. The oxide scale composed of both amorphous and crystalline silica was found also on the C-face oxidized for 20 h as shown in Fig. 3(e).

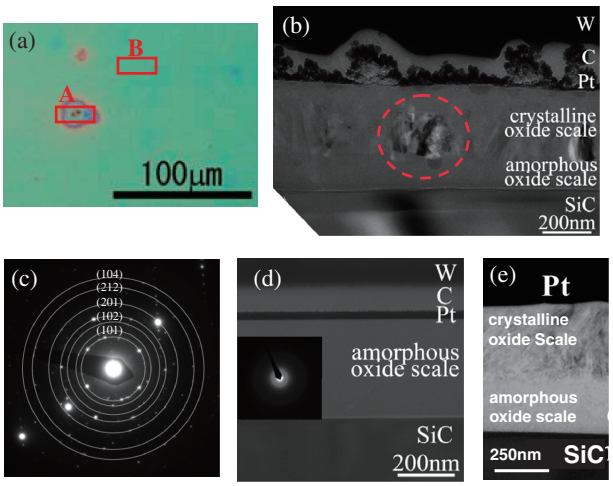

Fig. 3. (a) OM image of the sample after oxidized for 16 h, (b) cross-sectional TEM image of region A indicated in (a), (c) SADP of the circled region in (b), and (d) cross-sectional TEM images of region B indicated in (a). (e) The structure corresponding to (b) observed in C-face oxide scale.

Figure 4(a) shows an OM image of the Si-face of the sample oxidized for 25 h. The pattern formed on the surface of the sample was approximately 70 μm in size. Figure 4(b) shows cross-sectional TEM image from the specimen taken from the center of the pattern, as indicated by the arrow in Fig. 4(a). The thickness of the oxide scale varied greatly. The thickest part of the scale was about twice as thick as the surroundings, as shown in the right side of the image. Voids were observed in the crystalline scale close to the surface of the cross-sectional TEM specimen. Figure 4(c) is a schematic of the formed oxide scale. The oxide scale was crystalline phase from the surface to the scale/SiC interface in some regions. However, in other regions, the oxide scale was divided into two layers with crystalline phase on the upper and amorphous phase on the lower layer. This crystalline phase oxide scale was surrounded by a relatively thin uniform amorphous phase oxide scale. **Figures 5**(a)–5(f) shows results of XEDS elemental mapping from the region indicated by the broken line square in Fig. 4(b). Traces of calcium were found in the crystalline phase silica as shown in Fig. 5(d).

Figure 6 shows OM images of (a) the Si-face and (b) the C-face of the oxidized sample. The oxidation condition was 16 h at 1473 K in still air. The spherical patterns formed were not significantly different from the results of the oxidation in dry oxygen. **Figure 7** shows (a) OM image of one of the patterns formed on the Si-face of the sample, (b)–(d) cross-sectional TEM image corresponding to regions A, B and C in Fig. 7(a), respectively. The oxide scale in the center of the pattern (region A) was composed of crystalline phase silica, while the surrounding regions (regions B and C) were composed of amorphous phase silica. The surrounding amorphous phase oxide scales are roughly formed with non-uniform thickness. The oxide scales composed of only crystalline or amorphous phase were also observed on the C-face as shown in Figs. 7(e) and 7(f), respectively. The thickness of the scales are comparably uniform more than that on the Si-face.

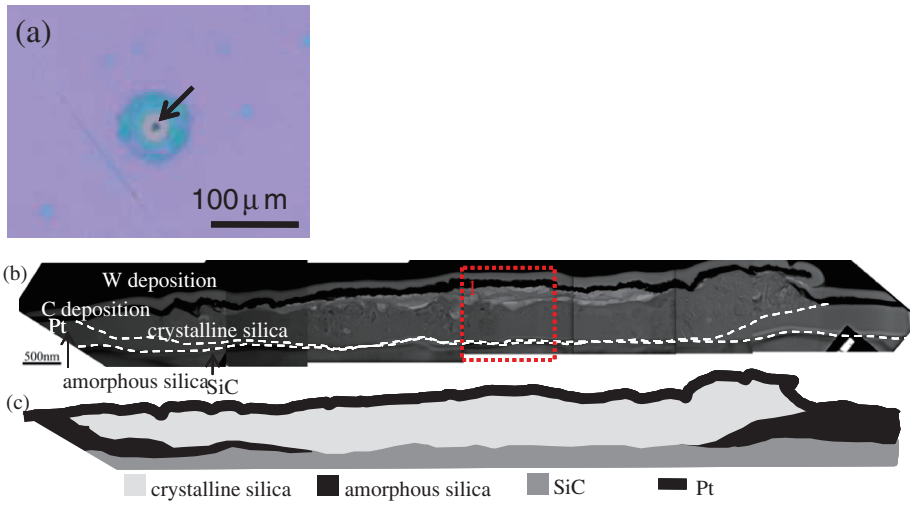

Fig. 4. (a) OM image of the sample oxidized for 25 h (b) cross-sectional TEM image of the center of the pattern indicated by the arrow in (a), and (c) schematic of (b).

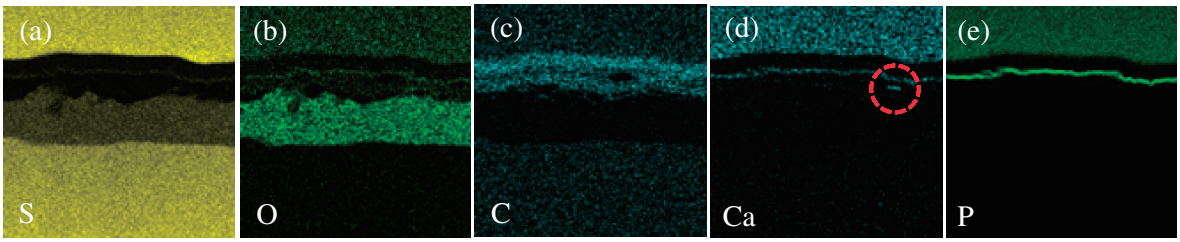

Fig. 5. (a)–(e) XEDS elemental mapping of Si, O, C, Ca, and Pt corresponding to the region indicated in Fig. 4(b), respectively.

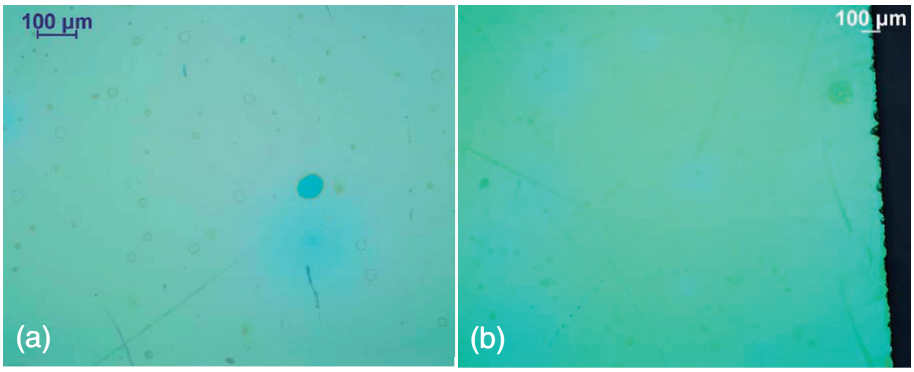

Fig. 6. OM images of (a) Si-face and (b) C-face of the sample oxidized in air for 16 h.

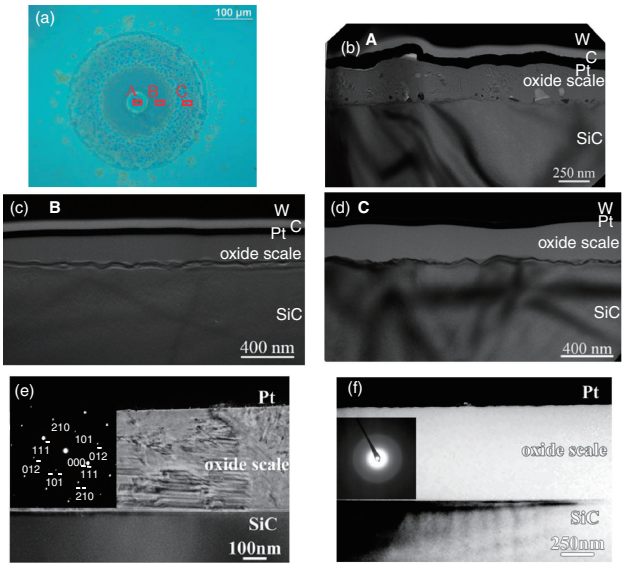

Fig. 7. (a) OM image of the sample oxidized for 16 h in air, (b)–(d) Cross-sectional TEM image of region A, B and C, respectively. (e) and (f) Cross-sectional TEM images of C-face crystalline and amorphous scale with the uniform interface compared to Si-face (b)–(d), respectively. The insets show the corresponding SADPs of the scales in (e) and (f), respectively.

4. Discussion

Many studies have reported the morphology of the formed crystalline oxide scales as radialite, a disk-shaped crystalline with characteristic dendritic cracks.[3),9)] These cracks which formed in the radialites are said to be caused by volume contraction due to the transformation from beta-cristobalite to alpha-cristobalite, which is the transformation from cubic to tetragonal structure that occurs during the cooling process.[10)] From the identification by SADP in our study, the crystalline phase silica is believed to have undergone the phase transformation from beta phase to alpha phase. However, in our study the characteristic cracks were not found in the morphology of the crystalline oxide scales.

As our experiment was conducted at the relatively low temperature (1473 K) and short oxidation time (less than 25 h), the crystallization of the oxide scales most likely occurred at the early stage of the oxidation. The lack of these characteristic cracks, as mentioned earlier, may be due to the initial state of crystallization in this study. Pressure et al. reported that at the initial stage of crystallization, the characteristic hexagonal shape crystalline silica was found in experiments conducted at high temperature (1673 K) and longer oxidation time (28 h).[9)] However, despite the early stage of the crystallization in our study, the crystalline oxide scales formed were not hexagonal shaped, but rather round with rough edges, as shown in Fig. 1(a)–1(c). It has been discussed in many studies that the nucleation of the crystalline silica is likely to form at inhomogeneous areas of the surface of the sample, such as over surface scratches or around the edges of the sample.[9),11)] But our results show that the crystallization occurred randomly, and did not concentrate around the edges of the samples, and as shown in Fig. 1(c), and did not grow along the scratch that existed prior to the oxidation. Even though the spherical patterns were observed near the scratch, the crystallization was not centered over the scratch.

The oxidation temperature, oxidation time, additives (especially in case of sintered silicon carbide), impurities and surface morphology are believed to be the influencing factors for the crystallization of the amorphous silica.[11)] From our results, the crystallization was not formed over the scratch. However, traces of calcium were found in the crystalline oxide scale. Therefore, we believe that impurities, calcium in this case, have a stronger influence on the nucleation of the crystallization than the surface morphology. A study by Frischat reported that the diffusion of

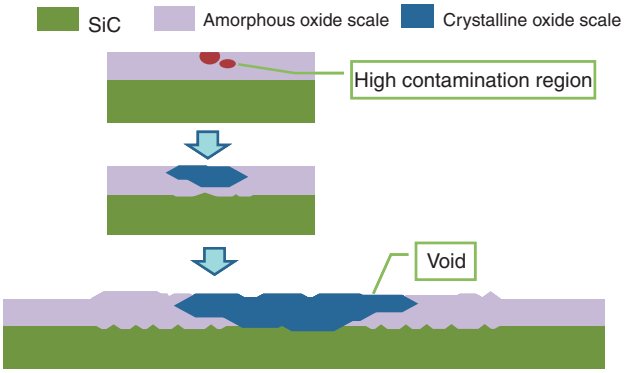

Fig. 8. Schematic of crystallization progress.

calcium in silica glass is higher than the diffusion of oxygen at the same temperature.[12] Considering the concentration of calcium and the diffusion rate reported for calcium in silica glass, we believe that the calcium contamination was in the SiC sample as aggregations or highly concentrated on the surface of the sample prior to the thermal oxidation. This agrees well with a study made by Bruckner which concluded that the concentration of the contamination must be sufficient in order for it to become the crystallization center of the vitreous silica.[13] However, the origin of the calcium contamination found in our study still remains unclear.

From comparative studies of oxidation in air, it was found that the change of oxidation environment has a small influence on the crystallization. From the observation of where crystalline phase oxide scales divided into two layers, one possible interpretation is that the crystalline scale grows much faster laterally than into the bulk. The lateral growth rate can be roughly estimated to be at least 30 times faster than the growth rate into the bulk. The result in this study agrees well with the study of Opila in 1999[14] who observed that the effect of impurities is much stronger than water vapor in the oxidation atmosphere. Our results show that impurities have more influence on the crystallization than the surface morphologies or the oxidation environment. The microstructures of the scale on both the Si-face and the C-face were completely identical except the roughness of SiC/scale interface and the thickness as a function of oxidation time. The difference could be related to the difference of the oxidation mechanism at the SiC/scale interface on the Si-face and the C-face, which will be discussed elsewhere[15] in detail, however, the crystallization of the amorphous scale was originated at the surface of the scale which was enough far away from the SiC/scale interface.

From the observed results of various stages of crystallization, the crystallization process is modeled schematically as shown in **Fig. 8**. The crystallization is believed to occur with the following steps; the first formed oxide scale was amorphous phase silica. It created a dense oxide scale cover of uniform thickness over all the surfaces of the SiC. Regions with a high density of contamination (calcium in this study) existed in the amorphous oxide scale (or possibly over the surface). The nucleation of the crystallization starts at the region with a high density of contamination, because the impurity is believed to decrease the average Si–O–Si chain length and disruption of the rings in vitreous silica. As a result, the crystallization easily occurs in the regions where the density of contaminations is sufficiently high. The crystalline phase continued to grow. However, these crystalline layers might contain some voids, which probably occur due to the structure modification of the crystallization. In the vicinity of the center of the crystalline scale, the crystalline phase may reach to the silica/SiC interface but overall, the lateral growth will be much faster than the bulk growth. For the surrounding regions, the crystalline phase oxide layer would remain as the upper layer over the amorphous oxide layer. The strains accumulated due to the crystallization might induce the roughening of the crystalline oxide scale and the surrounded amorphous oxide scale.

5. Summary

The Si-face of single crystal silicon carbide was oxidized in pure oxygen and in air at 1473 K for 9–25 h. The thermally formed oxide scales were composed mostly of amorphous silica with some crystalline phase oxide scales randomly distributed on the formed oxide scale. We characterized the microstructures of the thermally formed oxide scales using transmission electron microscopy with low-dose observation technique and X-ray energy dispersive spectroscopy. The crystalline oxide scale was identified by selected area diffraction patterns as alpha cristobalite. Traces of calcium were found where the crystalline phase oxide scale existed, which could be the nucleation site for the crystallization. Our results suggest that the control of impurities is more important than the surface morphology and the oxidation environment to form the uniform amorphous oxide layer on single crystal SiC.

References

1) W. L. Vaughn and H. G. Maahs, *J. Am. Ceram. Soc.*, 73, 1540–1543 (1990).
2) A. H. Heuer, L. U. Ogbuji and T. E. Mitchell, *J. Am. Ceram. Soc.*, 63, 354–355 (1980).
3) T. Narushima, T. Goto and T. Hirai, *J. Am. Ceram. Soc.*, 72, 1386–1390 (1989).
4) L. U. J. T. Ogbuji and M. Singh, *J. Mater. Res.*, 10, 3232–3240 (1995).
5) L. U. J. T. Ogbuji, *J. Am. Ceram. Soc.*, 80, 1544–1550 (1997).
6) D. S. Fox, *J. Am. Ceram. Soc.*, 81, 945–950 (1998).
7) M. J.-F. Guinel and M. G. Norton, *J. Mater. Res.*, 21, 2550–2563 (2006).
8) E. Opila, *J. Am. Ceram. Soc.*, 78, 1107–1110 (1995).
9) V. Pressure, A. Loges, Y. Hemberger and K. G. Nickel, *J. Am. Ceram. Soc.*, 92, 724–731 (2009).
10) W. D. Kingery, "Introduction to Ceramics", Wiley (1960).
11) V. Pressure and K. G. Nickel, *Crit. Rev. Solid State Mater. Sci.*, 33, 1–99 (2008).
12) G. H. Frischat, *J. Am. Ceram. Soc.*, 52, 625 (1969).
13) R. Bruckner, *J. Non-Cryst. Solids*, 5, 123–175 (1970).
14) E. J. Opila, *J. Am. Ceram. Soc.*, 82, 625–636 (1999).
15) B. Chayasombat, T. Kato, T. Hirayama, T. Tokunaga, K. Sasaki and K. Kuroda, *J. Ceram. Soc. Jpn.*, to be submitted.